EFFECT OF BRAGG INTERBAND TRANSITIONS ON THE DIELECTRIC CONSTANT OF METALS

A. I. GOLOVASHKIN and G. P. MOTULEVICH

P. N. Lebedev Physics Institute, U.S.S.R. Academy of Sciences

Submitted April 30, 1969

Zh. Eksp. Teor. Fiz. 57, 1054–1063 (September 1969)

The complex dielectric constant connected with the Bragg interband transitions is calculated. The results are compared with the experimental data for the interband dielectric constant and interband conductivity of a number of metals. The contribution of the Bragg interband transitions to the dielectric constant at low frequencies is determined for aluminum, lead, and indium. The contribution is of the order of 10–100.

To obtain the characteristics of the conduction electrons of metals and alloys by an optical method, one uses the results of measurements of the optical constants in the long-wave region of the spectrum, i.e., in that region where the real interband transitions can be neglected. However, even in this region there is a strong influence of the virtual interband transitions on the dielectric constant. It greatly exceeds the corresponding influence in dielectrics, since in metals there exists for a large number of electrons energy gaps of the order of 0.1–1 eV, which is smaller by a factor 10–100 than the gaps in dielectrics. These gaps in metals are connected with Bragg planes.

In this paper we determine the contribution of the Bragg interband transitions to the complex dielectric constant of metals. We show that the contribution of the virtual interband transitions to the real part of the dielectric constant of the metals reaches a value ~10–100 in the long-wave region. For alloys and transition metals, for which the effective collision frequencies of the conduction electrons are large, the indicated virtual transitions exert a strong influence on the optical properties.[1,2]

INTERBAND TRANSITIONS CONNECTED WITH BRAGG PLANES[1)]

As is well known,[4] the linear polarizability of a quantum-mechanical system can be represented in the form

$$\chi_{ik}(\omega)=\sum_{n,m}[\rho_0(E_n)-\rho_0(E_m)]\frac{(d_i)_{nm}(d_k)_{mn}}{E_n-E_m+\hbar\omega+i\hbar\nu}. \qquad (1)$$

Here χ_{ik} is the linear polarizability tensor, E_n and E_m are the energy levels of the system unperturbed by the external field, $(d_i)_{nm}$ is the matrix element of the i-th component of the dipole moment per unit volume, $(\rho_0)_{nm}=\delta_{nm}\rho_0(E_n)$ is the density matrix of the unperturbed system, δ_{nm} is the Kronecker symbol, $\hbar\omega$ is the energy of the quantum of incident light, and $1/\nu$ is the relaxation time.

Formula (1) is obtained by the kinetic-equation method for the density matrix in the relaxation-time approximation. The Hamiltonian of the interaction is taken in the dipole approximation.

Let us apply formula (1) to interband transitions connected with Bragg planes. Being interested principally in polyvalent metals, we assume that the Bragg plane intersects the sphere of the free electrons.[2)] We assume that the planes act independently. Confining ourselves to transitions to the closest unfilled band, we denote the lower band by the index 1 and the upper one by 2. Starting from the weak-coupling approximation, we assume that the wave functions of the electrons are equal to a sum of two plane waves whose wave vectors differ by an amount equal to the reciprocal-lattice vector. A comparison with experiment, which will be reported later, shows that this model agrees sufficiently well with the real situation.

In a metal, the sum over n and m in (1) includes both summation with respect to the lower and upper states for each electron and summation over all the electrons, i.e.,

$$\sum_{n,m}\to\sum_{i}\sum_{n=1}^{2}\sum_{m=1}^{2}\int 2d^3p/(2\pi\hbar)^3.$$

The integration is carried out over the entire volume enclosed by the Fermi surface.

For the wave functions ψ_n of the electron in the lower and upper bands (n = 1, 2) we have the expressions:[5]

$$\psi_n=a_n^{(1)}\exp(i\mathbf{pr}/\hbar)+a_n^{(2)}\exp[i(\mathbf{p}-2\mathbf{p}_g)\mathbf{r}/\hbar], \qquad (2)$$

$$a_n^{(1)}=2^{-1/2}(1+X^2+(-1)^nX\sqrt{1+X^2})^{-1/2}, \qquad (3)$$

$$a_n^{(2)}=a_n^{(1)}(X+(-1)^n\sqrt{1+X^2}), \qquad (4)$$

$$X=\frac{p_g}{m|V_g|}(p_g-p_\perp). \qquad (5)$$

Here $p_\perp$ is the projection of the momentum $\mathbf{p}$ on the normal to the Bragg plane, $\mathbf{p}_g$ is a vector perpendicu-

[1)] A more complete derivation of all the formulas, together with the results of numerical calculations, is given in [3].

[2)] We do not consider in this paper the case when the Bragg plane does not intersect the free-electron sphere, as is the case, for example, for metals of the first group. It is easy to generalize the results to include this case, too.

lar to the Bragg plane, p_g is equal to the distance from the center of zone Γ to the Bragg plane, V_g is the Fourier component of the pseudopotential and corresponds to the given Bragg plane, and m is the mass of the free electron.

The energy difference between the upper and lower bands can be represented in the form

$$E_2 - E_1 = \Delta E = \hbar\omega_g\sqrt{1+X^2}. \tag{6}$$

Here $\hbar\omega_g = 2|V_g|$.

The matrix element of the dipole moment is

$$(d_i)_{nm} = \frac{e\hbar}{im\Delta E}(p_i)_{nm}. \tag{7}$$

Using the wave functions (2)–(4), we get

$$p_{12} = p_g(1+X^2)^{-1/2}. \tag{8}$$

From the expression obtained for the momentum matrix element it follows that the interband transitions produce only an electric field having a component perpendicular to the atomic planes corresponding to the Bragg plane. The polarization vector connected with the indicated transitions is also perpendicular to the atomic planes.

For electrons in a metal, $\rho_0(E)$ is a function of the Fermi distribution. Since $\Delta E \gg kT$, we get $\rho_0(E_2) - \rho_0(E_1) = 1$ for the points of the ring produced in the reduced-band scheme by the intersection of the Fermi surface with the plane x = const, and is equal to zero outside this ring, see Fig. 1. Thus, $d^3p = Sdp_\perp$, where the area of the ring is

$$S = 2\pi m\hbar\omega_g\sqrt{1+X^2}. \tag{9}$$

For the linear polarizability connected with one Bragg plane, we obtain from (1)

$$\chi_g = \frac{e^2}{4\pi^2\hbar^2}\frac{p_g}{\omega_g}I, \tag{10}$$

$$I = \int_0^\infty \frac{dX}{(1+X^2)^{3/2}}\left(\frac{1}{\sqrt{1+X^2}-\omega'-i\nu'} + \frac{1}{\sqrt{1+X^2}+\omega'+i\nu'}\right). \tag{11}$$

Here $\omega' = \omega/\omega_g$ and $\nu' = \nu/\omega_g$. The upper limit can be taken at infinity, since we assume that $p_g(2p_g - p_F)/m|V_g| \gg \nu'$, where p_F is the rings of the sphere of the free electrons at a concentration equal to the valence concentration. The quantities I, ω', ν', and ν should have an index g, since they are different for physically non-equivalent Bragg planes. We shall omit the index g whenever this does not lead to confusion.

Let us take an arbitrary system of rectangular coordinates and consider a crystal of arbitrary symmetry. We renumber all the physically equivalent Bragg planes, introducing the index G. For different systems of physically equivalent Bragg planes, we use the index g. In terms of this notation

$$\chi_{ik} = \sum_g \chi_{ik}^{(g)} = \sum_g \chi_g \sum_G (\mathbf{s}_{gG}\mathbf{a}_i)(\mathbf{s}_{gG}\mathbf{a}_k). \tag{12}$$

Here $\mathbf{s}_{gG}$ is the unit vector normal to the atomic planes corresponding to the Bragg plane G from the system of planes g; $\mathbf{a}_i$ is the unit vector of the i-th coordinate axis. For a cubic crystal

$$\chi_{ik}^{(g)} = \frac{e^2}{12\pi^2\hbar^2}\frac{n_g p_g}{\omega_g} I_g \delta_{ik}, \tag{13}$$

where n_g is the number of physically equivalent Bragg planes. We confine ourselves below to cubic crystals only.

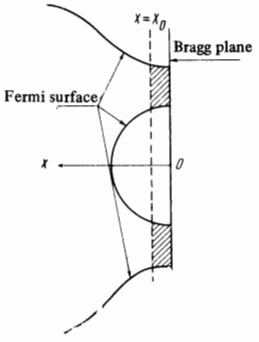

FIG. 1

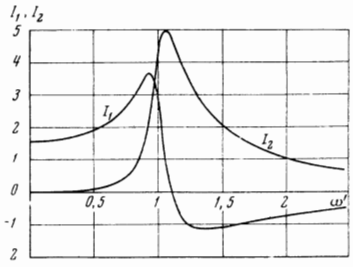

FIG. 2

FIG. 1. Intersection of the Fermi surface and a Bragg plane. The shaded section represents the phase volume of the electrons for which the energy gap is $\Delta E \leqslant \hbar\omega_g + \hbar\nu$.

FIG. 2. The functions $I_1(\omega')$ and $I_2(\omega')$ at $\nu' = 0.1$.

Let us consider the action of a system of physically equivalent Bragg planes. The contribution of the interband transitions near these planes to the complex dielectric constant ϵ' is determined by the formulas

$$\varepsilon' = 4\pi\chi = \varepsilon - i\frac{4\pi\sigma}{\omega}, \tag{14}$$

$$\varepsilon = \frac{e^2}{3\pi\hbar^2}\frac{n_g p_g}{\omega_g} I_1, \tag{15}$$

$$\sigma = \frac{e^2}{12\pi^2\hbar^2} n_g p_g I_2, \tag{16}$$

$$I_1 = \int_0^\infty \frac{(\sqrt{1+X^2}-\omega')\,dX}{(1+X^2)^{3/2}[(\sqrt{1+X^2}-\omega')^2+\nu'^2]} + \int_0^\infty \frac{(\sqrt{1+X^2}+\omega')\,dX}{(1+X^2)^{3/2}[(\sqrt{1+X^2}+\omega')^2+\nu'^2]}, \tag{17}$$

$$I_2 = \omega'\nu'\left\{\int_0^\infty \frac{dX}{(1+X^2)^{3/2}[(\sqrt{1+X^2}-\omega')^2+\nu'^2]} - \int_0^\infty \frac{dX}{(1+X^2)^{3/2}[(\sqrt{1+X^2}+\omega')^2+\nu'^2]}\right\}. \tag{18}$$

An expression for the interband conductivity σ was obtained in [5]. It differs somewhat from the expression obtained in the present paper. The difference is connected with the fact that in [5] we used an interaction Hamiltonian $H = (g/mc)\mathbf{p}\cdot\mathbf{A}$, where $\mathbf{A}$ is the vector potential of the electromagnetic field. Terms of order $\mathbf{A}^2$ were neglected, so that the expressions obtained in [5] do not hold when $\omega' < 1 - \nu'$. In the region $\omega' \gtrsim 1$, the two expressions are close to each other. In addition, in [5] they discarded the second term in the integral I_2, which is immaterial for σ. However, failure to take into account the analogous term in ε leads to an appreciable error.

The dependence of the integrals (17) and (18) and the frequency ω' at values of the parameter $\nu' = 0.1$ is shown in Fig. 2. The increase of ν' leads to a decrease

and broadening of the maxima, leaving the general form of the curves unchanged.

The asymptotic behavior of the function $I_1(\omega')$ is given by

$$I_1(\omega')=\begin{cases}-\dfrac{\pi}{\omega'^2} & \text{if} \quad \omega'\gg 1\\ \dfrac{\pi}{\omega'^2}\left(1-\dfrac{1}{\sqrt{1+\nu'^2}}\right) & \text{if} \quad \omega'=0.\end{cases} \tag{19}$$

At small values of ν', the quantity $I_1(0)$ is practically constant, and equals[3] $\pi/2$. It is seen from Fig. 2 that near $\omega' = 1$ the function $I_1(\omega')$ is close to a step function, and the function $I_2(\omega')$ has a maximum. In the region $\omega' < \omega_{max}$ the function is practically linear over a wide range of I_2.[4]

Curve 1 of Fig. 3 shows the frequency ω'_{max} corresponding to the maximum of I_2 as a function of ν'. The shift of the position of the maximum of I_2 from a value equal to unity increases with increasing ν'.[5] The dependence of ω'_{max} on ν' is almost linear and in the region $\nu' \approx 0.1$–0.2 the shift amounts to 5–10%. Using Fig. 3, we can determine the value of $|V_g| = 0.5\hbar\omega_{max}/\omega'_{max}$.

Curve 2 of Fig. 3 gives the dependence of the maximum value of I_2 on ν'. With the aid of this plot it is possible to compare the experimental and theoretical absolute values of σ_{max}. When $\nu' \ll 1$ we have $I_2 \approx 0$. The asymptotic behavior of the function $I_2(\omega')$ at $\omega' \gg 1$ is given by[6]

$$I_2(\omega')=\frac{\pi}{\omega'^2},$$

which leads to the same $\sigma(\omega')$ dependence as obtained in [5].

The proportionality of ϵ and σ to the quantity ω^{-2} at high frequencies should naturally from physical considerations. At such frequencies, all the electrons are free, and we should obtain the usual Drude formulas. It is easy to obtain expressions for ϵ and σ in the absence of relaxation. Taking the limit at $\nu' \to 0$, we obtain

$$\varepsilon=\begin{cases}\dfrac{1}{3}\dfrac{e^2}{\hbar^2}\dfrac{n_g p_g}{\omega_g}\dfrac{1}{\omega'^2}\left(\dfrac{1}{\sqrt{1-\omega'^2}}-1\right) & \text{if} \quad \omega'<1,\\ -\dfrac{1}{3}\dfrac{e^2}{\hbar^2}\dfrac{n_g p_g}{\omega_g}\dfrac{1}{\omega'^2} & \text{if} \quad \omega'>1,\end{cases} \tag{20}$$

$$\sigma=\begin{cases}0 & \text{if} \quad \omega'<1,\\ \dfrac{1}{12}\dfrac{e^2}{\pi\hbar^2}n_g p_g\dfrac{1}{\omega'\sqrt{\omega'^2-1}} & \text{if} \quad \omega'>1.\end{cases} \tag{21}$$

Using the asymptotic behavior, as $\omega' \to \infty$, of the dielectric constant pertaining both to the conduction electrons and to the interband transitions, we can obtain the following relation, which is equivalent to the sum rule:

$$\frac{m}{12\pi\hbar^2}\sum_g n_g p_g \omega_g = N_{val} - N. \tag{22}$$

The summation extends here over all effective Bragg planes intersecting the free-electron sphere.

In determining the contribution of the interband transitions to the dielectric constant at low frequencies, it is convenient to use the following formula:

$$\varepsilon(\omega')=\frac{4\pi}{\omega_g}I_1(\omega')\frac{\sigma_{max}}{I_{2\,max}}. \tag{23}$$

Here σ_{max} and $I_{2\,max}$ are the maximum values of σ and I_2 at a given ν'. The use of this formula requires no identification of the observed band of the interband conductivity σ.

Calculations show that the following relation obtains between the jump of the dielectric constant $\epsilon_{max} - \epsilon_{min}$ and the maximum value of the conductivity σ_{max} pertaining to the given interband transition:

$$\frac{\omega_g}{4\pi}\frac{\varepsilon_{max}-\varepsilon_{min}}{\sigma_{max}} \equiv \frac{I_{1\,max}-I_{1\,min}}{I_{2\,max}} \approx 0.95. \tag{24}$$

Relation (24) is valid when $0.04 < \nu' < 0.6$. A more exact formula for the quantities $(I_{1\,max} - I_{1\,min})/I_{2\,max}$ is given in [3].

The results enable us to determine ν' from the shape of the experimental plot of $\sigma(\omega)$. To this end, it is necessary to choose ν' such as to obtain the best agreement between the theoretical contour and the experimental band. Since this is a very laborious task, we can use a simpler but less exact method, in which ν' is determined from the value of the frequency ω_α corresponding to the quantity $\sigma(\omega_\alpha) = \alpha\sigma_{max}$. Figure 4 shows the dependence of ν' on the quantity $1 - \omega_\alpha/\omega_{max}$ (here $\omega_\alpha < \omega_{max}$). Curve 1 corresponds to $\alpha = 0.5$ and curve 2 to $\alpha = 0.7$. If the investigated band is well iso-

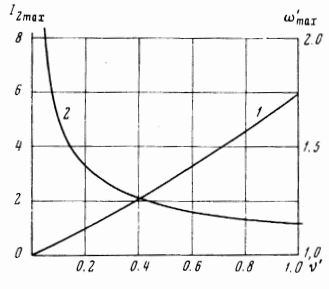

FIG. 3. Dependence of the frequency shift corresponding to the maximum interband conductivity (curve 1) and the maximum value of the integral I_2 (curve 2) on ν'.

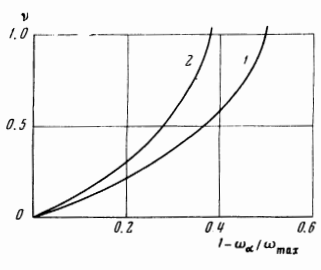

FIG. 4. Illustrating the determination of ν' from the shape of the interband-conductivity band. Curve 1 – $\alpha = 0.5$; curve 2 – $\alpha = 0.7$.

[3] We note that the two integrals in I_1 make approximately equal contributions at low frequencies.

[4] Although the dependence of I_2 on ω' is steep in this region, extrapolation of this dependence to zero values of I_2 gives a value of ω' much smaller than unity. (This means that the threshold frequency ω_{thr} is much lower than ω_g.) The difference increases with increasing ν'.

[5] In [5] we also determined the indicated shift of the maximum as a function of the level broadening γ'. For small ν', corresponding to small γ', the shifts practically coincide. At larger values, however, a difference is observed. In [6] we obtained too low a shift, owing to the factors discussed above.

[6] When $\omega' \gg 1$ the integrals I_1 and I_2 do not depend on ν', which is perfectly natural, since the relaxation processes can be neglected at high frequencies (it is assumed that $\nu' \lesssim 1$).

lated from the other interband transitions, then we can use any curve. When several bands are superimposed, it is necessary to use the curve corresponding to the least distorted part of the investigated band.

In concluding this section, let us estimate the number of electrons that determine the interband-conductivity band near the maximum. We take into account the electrons from which the energy gap is $\Delta E \leq \hbar\omega_g + \hbar\nu$. It is obvious that these electrons are contained in the volume shown cross hatched in Fig. 1. The concentration of such electrons, when account is taken of one Bragg plane G from the system planes g, is equal to

$$N_{gG} = \frac{m^2}{4\pi^2\hbar}\frac{\omega_g^2}{p_g}\int_0^{X_0} dX\sqrt{1+X^2}, \qquad (25)$$

where $X_0 = \sqrt{2\nu'_g}\sqrt{1+0.5\nu'_g}$. An estimate of this quantity for lead at $T = 4.2^\circ K$ yields the values $N_{111,G} \approx 7\times10^{20}$ cm^{-3} and $N_{200,G} \approx 5\times10^{20}$ cm^{-3}. Since the concentration of the valence electrons for lead $N_{val} = 1.34\times10^{23}$ cm^{-3} we see that $N_{gG} \ll N_{val}$. In other words, different electrons take part in the interband Bragg transitions connected with different planes.

COMPARISON WITH EXPERIMENT

Let us compare the results with experiment. In the visible and the near infrared regions, experiment reveals for metals bands of interband conductivity, which can be set in correspondence with bands associated with Bragg planes.[6-8] For a comparison of the form of the experimental and theoretical bands it is convenient to use the {200} band of aluminum. This band is sufficiently far from the other bands and lies in the region where the contribution of the conduction electrons is small.

Figure 5 shows the comparison of the experimental and theoretical shapes of the {200} band of aluminum. We see that the experimental points obtained on the basis of [8] agrees sufficiently well with the theoretical curve. For the indicated band, $\nu'_{200} = 0.13$.

We have determined from the data of [6-8], for the experimentally obtained bands, the Fourier components of the pseudopotential V_g. They turned out to be much smaller than the corresponding components determined in [5]. In addition, the experimental shape of the bands was used to determine the effective collision frequencies ν'_g. From the values of V_g and ν'_g we calculated $\sigma_{g\,max}$. The latter are compared with the experimental values of $\sigma_{g\,max}$ in Table I.[7] It follows from this table that the theoretical values of $\sigma_{g\,max}$ for the principal bands of the interband conductivity exceed the experimental ones by a factor 1.5–2.[8]

The disparity obtained in this paper between experiment and theory may be due to the following. The wave function of the electron can be represented as a sum of two plane waves only in first approximation. The use of a more accurate wave function leads to a dependence of the energy gap not only on $p_\perp$ but also on $p_\parallel$. Allowance for this dependence leads to a decrease of the theoretical value of σ. This circumstance is particularly important in the region of intersection of several Bragg planes.

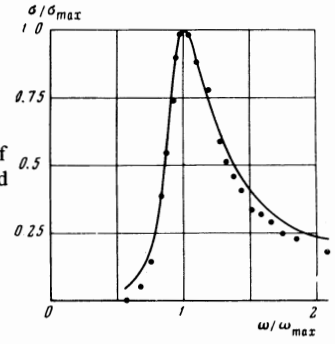

FIG. 5. Comparison of the experimental and theoretical shapes of the {200} band of aluminum. Solid line – theoretical curve at $\nu'_{200} = 0.13$; points – experimental values.

Table I. Comparison of theoretical and experimental values of σ_{max}

Metal	T, °K	Band indices (g)	$\hbar\omega_{max}$, eV	ν'	$\lvert V_g\rvert$, eV	σ_{max} 10^{14} sec^{-1} theor	exp
Al	295	200	1.50	0.13	0.70	73	47
Pb	4.2	111	2.07	0.11	0.97	77	32
		200	1.48	0.24	0.64	41	13
	78	111	2.14	0.16	0.98	61	29
		200	1.38	0.25	0.60	40	12
	293	111	2.24	0.26	0.96	45	28
		200	1.08	0.44	0.42	28	12
In	4.2	111	1.48	0.23	0.65	51	34
		200	0.60	0.38	0.24	33	30
	295	111	1.26	0.31	0.53	42	26
		200*	0.56	0.40	0.22	31	22

* In the determination of ν' for this band, we took into account the fact that in the region 0.3 – 0.4 eV there is an additional contribution of the interband transitions, not connected with this Bragg plane.

Table II

Metal	T, °K	$\frac{m}{12\pi\hbar^2}\Sigma n_g p_g \omega_g$, 10^{22} cm^{-3}	$N_{val} - N$, 10^{22} cm^{-3}
Al	295	6.0	8.7
Pb	4.2	9.5	9.7
	78	9.2	9.5
	293	8.2	9.1
In	4.2	5.5	5.4
	295	4.7	4.3

Let us compare the sum rule (22) with experiment. The results of such a comparison, given in Table II, show that for Pb and In formula (22) is satisfied at all temperatures. Thus, there are no significant interband transitions in these metals, other than those considered. For Al, the contribution from these transitions is somewhat smaller than the difference $N_{val} - N$. The reason for this is not yet clear.

Let us examine the connection between the jump $\Delta\epsilon = \epsilon_{max} - \epsilon_{min}$ and σ_{max}. In the presence of several close bands, the values of ϵ_g overlap, making the separation of $\Delta\epsilon$ difficult. However, it is possible to separate the jump $\Delta\epsilon$ for tin and lead at $T = 78^\circ K$. We then obtain

[7] In [5], an error has crept in the numerical calculation of the coefficient $(1/12)e^2/\pi^2\hbar^2$. All the calculated values of $\sigma_{g\,max}$ in [5,7] must be multiplied by 4.

[8] A theory based on allowance for the transitions near the symmetry points leads to theoretical values that are lower than the experimental ones by a factor 5 – 10 [9].

$$\frac{\omega_g}{4\pi}\frac{\varepsilon_{max}-\varepsilon_{min}}{\sigma_{max}} = \begin{cases} 0.7 & \text{for Sn} \\ 0.8 & \text{for Pb.} \end{cases}$$

The obtained values are in good agreement with the theoretical value 0.95.

It follows from the considered theory that for anisotropic single crystals the different bands σ_g are excited by light of different polarization. This was observed for Zn and Mg single crystals.[10-12] This circumstance is used to identify the bands.

On the whole, it can be assumed that the experiment confirms well the model under consideration.

Let us calculate the contributions of the virtual interband transitions to the dielectric constant at low frequencies. The results of such a calculation are given in Table III. It is seen from Table III that the contribution

Table III. Contribution of the virtual interband transitions to the dielectric constant of a number of metals

Metal	T, °K	ε(0)
Al	295	26
Pb	4.2	9
	78	10
	293	15
In	4.2	45
	295	40

of the indicated transitions to ϵ is of the order of 10–100. If it is recognized that when $\nu_e \sim 10^{15}$ sec^{-1} the contribution of the conduction electron to the long-wave region is $\epsilon_e \sim 10^2$, it becomes clear that allowance for the virtual interband transitions is essential even in the long-wave region.

In conclusion, we are grateful to L. V. Keldysh for a number of valuable remarks made during the discussion of the present work.

[1] A. I. Golovashkin, I. S. Levchenko, and G. P. Motulevich, Zh. Eksp. Teor. Fiz. **57**, 74 (1969) [Sov. Phys.-JETP **30**, 44 (1970)].

[2] I. E. Leksina, G. P. Motulevich, A. A. Shubin, I. A. Baranov, V. A. Sytnikov, and R. S. Shmulevich, Fiz. Metal. Metalloved., in press.

[3] A. I. Golovashkin and G. P. Motulevich, FIAN Preprint No. 67, 1969.

[4] F. Seitz, Modern Theory of Solids, McGraw-Hill, 1940; E. Ehrenreich and M. H. Cohen, Phys. Rev. **115**, 786 (1959); A. V. Sokolov, Opticheskie svoĭstva metallov (Optical Properties of Metals), Fizmatgiz, 1961; M. I. Kaganov and I. M. Livshitz, Zh. Eksp. Teor. Fiz. **45**, 948 (1963) [Sov. Phys.-JETP **18**, 655 (1964)]; S. A. Akhmanov and R. V. Khokhlov, Problemy nelineĭnoĭ optiki (Problems of Nonlinear Optics), AN SSSR, 1964; V. M. Faĭn and Ya. I. Khanin, Kvantovaya Radiofizika (Quantum Radiophysics), Sov. Radio, 1965; J. Phillips, Optical Spectra of Solids.

[5] A. I. Golovashkin, A. I. Kopeliovich, and G. P. Motulevich, Zh. Eksp. Teor. Fiz. **53**, 2053 (1967) [Sov. Phys.-JETP **26**, 1161 (1968)]; ZhETF Pis. Red. **6**, 651 (1967) [JETP Lett. **6**, 142 (1967)].

[6] A. I. Golovashkin, I. S. Levchenko, G. P. Motulevich, and A. A. Shubin, Zh. Eksp. Teor. Fiz. **51**, 1622 (1966) [Sov. Phys.-JETP **24**, 1093 (1967)].

[7] A. I. Golovashkin and G. P. Motulevich, ibid. **53**, 1526 (1967) [**26**, 881 (1968)].

[8] I. N. Shklyarevskiĭ and R. G. Yarovan, Opt. Spektr. **16**, 85 (1964).

[9] J. C. Phillips, Optical Properties and Electronic Structure of Metals and Alloys, Proc. 1st Internat. Coll, Paris, 1965, F. Abeles, Ed., North-Holland, 1966, p. 22.

[10] A. H. Lettington, ibid. 1. 147.

[11] A. P. Lenham and D. M. Treherene, JOSA **56**, 752 (1966).

[12] D. Jones and A. H. Lettington, Proc. Phys. Soc. **92**, 948 (1967).

Translated by J. G. Adashko
121